

Cleaved and Etched Facet Nitride Laser Diodes

A. C. Abare, M. P. Mack, M. Hansen, R. K. Sink, P. Kozodoy, S. Keller,
J. S. Speck, J. E. Bowers, *Fellow, IEEE*, U. K. Mishra,
L. A. Coldren, *Fellow, IEEE*, and S. P. DenBaars

(Invited Paper)

Abstract—Room-temperature (RT) pulsed operation of blue (420 nm) nitride-based multiquantum-well laser diodes grown on a-plane and c-plane sapphire substrates has been demonstrated. Structures investigated include etched and cleaved facets as well as doped and undoped quantum wells. A combination of atmospheric and low-pressure metal organic chemical vapor deposition using a modified two-flow horizontal reactor was employed. Threshold current densities as low as 12.6 kA/cm^2 were observed for $10 \times 1200 \text{ }\mu\text{m}$ lasers with uncoated reactive ion etched facets on c-plane sapphire. Cleaved facet lasers were also demonstrated with similar performance on a-plane sapphire. Laser diodes tested under pulsed conditions operated up to 6 h at RT. Lasing was achieved up to $95 \text{ }^\circ\text{C}$ and up to a 150-ns pulselength (RT). Threshold current increased with temperature with a characteristic temperature T_0 of 114 K.

Index Terms—Blue, diode, InGaN, GaN, laser, nitride, MQW, pulsed, room temperature.

I. INTRODUCTION

SEVERAL RESEARCH groups have demonstrated nitride based laser diodes [1]–[9]. This device is desirable for optical storage systems (e.g., high-density digital versatile disk, HD-DVD), printing, display technology, medical surgery and chemical monitoring (such as pollution). The lifetime estimate of 10 000 h from Nakamura at Nichia Chemicals, Inc., demonstrates the viability of these devices for commercial products [10].

Various approaches have been explored for fabricating nitride laser diodes. Sapphire substrates are used primarily due to the availability of low-cost high-quality wafers. [1]–[3], [6]–[9] C-plane sapphire is the primary orientation employed and has been used to fabricate devices with dry etched facets [1], [6], [7], [9] as well as cleaved facets [2], [8]. A-plane sapphire has been employed for fabricating cleaved facet laser diodes [1], [11]. Silicon carbide substrates, employing cleaved facets, are favored due to a closer lattice match and higher thermal conductivity [4], [5]. Their use is limited by the high cost of

Manuscript received February 20, 1998; revised April 14, 1998. The work of G. Meyer was supported by LLNL. The work of A. Husain was supported by the Defense Advanced Research Projects Agency. The work of J. Zavada was supported by the National Science Foundation and by the ARO. The work of M. Yoder, C. Wood, Y.-S. Park was supported by the Office of Naval Research.

A. C. Abare, M. Hansen, R. K. Sink, P. Kozodoy, S. Keller, J. S. Speck, J. E. Bowers, U. K. Mishra, L. A. Coldren, and S. P. DenBaars are with the Electrical and Computer Engineering Department and Materials Department, University of California, Santa Barbara, Santa Barbara, CA 93106 USA.

M. P. Mack is with Wright Laboratories, Wright Patterson Air Force Base, Dayton, OH 45433-7322 USA.

Publisher Item Identifier S 1077-260X(98)05438-0.

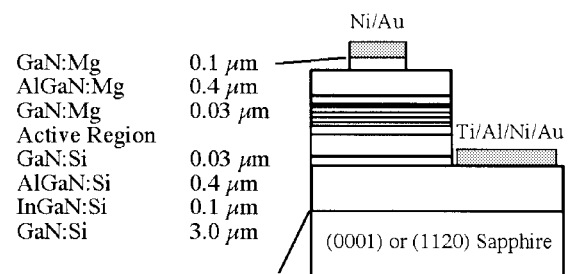


Fig. 1. Epitaxial layer structure and contacting scheme for laser diodes.

this substrate. In this paper, we report on the properties of laser diodes fabricated using reactive ion etched (RIE) facets on c-plane sapphire and cleaved facets on a-plane sapphire. We have also investigated the use of silicon doping in the quantum wells for the etched facet lasers.

II. EXPERIMENTAL

All samples were grown in a modified two-flow horizontal reactor (Thomas Swan, Ltd.) on a-plane (11 $\bar{2}$ 0) or c-plane (0001) sapphire substrates using a combination of atmospheric and low pressure metal-organic chemical vapor deposition (MOCVD). The chemical precursors used were trimethylgallium (TMGa), trimethylaluminum (TMAI), trimethylindium (TMIIn), bis(cyclopentadienyl) magnesium (Cp_2Mg), disilane (Si_2H_6), and ammonia (NH_3).

The general laser structure is shown in Fig. 1. Several device structures were grown exploring quantum-well doping and use of cleaved versus etched facets. The active region consists of ten 2.4-nm $\text{In}_{0.18}\text{Ga}_{0.82}\text{N}$ quantum wells. Structures with and without silicon doping in the wells were grown on c-plane sapphire. The samples with silicon doped quantum wells were grown on a- and c-plane sapphire. The barriers are 6 nm $\text{In}_{0.06}\text{Ga}_{0.94}\text{N}$ doped with silicon. The structures used 0.4- μm AlGaIn cladding regions surrounding this InGaIn MQW active region. X_{Al} was 0.06 for the majority of the structures. A GaN:Mg layer is used for a contact layer and an InGaIn:Si layer beneath the lower AlGaIn:Si cladding is used as a compliance layer [1].

The processing used Cl_2 RIE to form 125- μm -wide mesas. For the c-plane structure, the facets were also formed during this etch with mesa lengths ranging from 400 to 2000 μm . Facets for the a-plane structure were formed by cleaving along the (1 $\bar{1}$ 02) r-planes of the thinned (50 μm) sapphire substrate. N-contacts were formed surrounding this mesa. P-contact

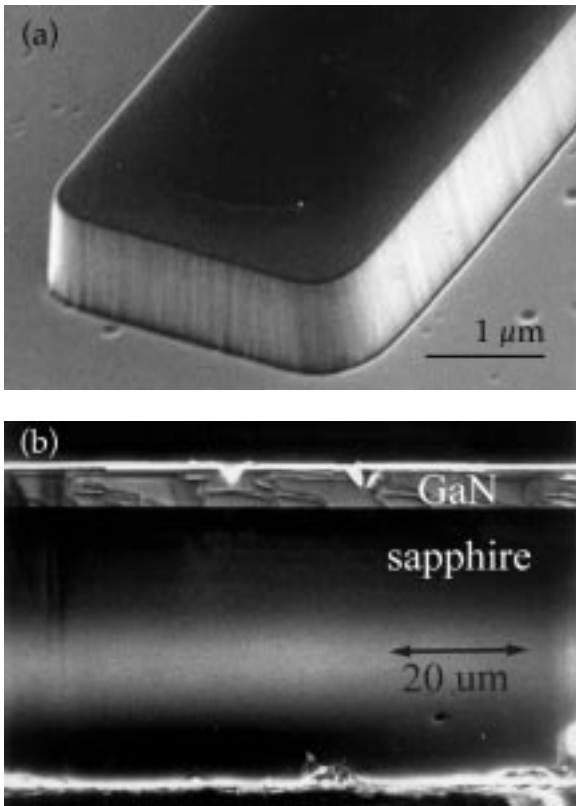


Fig. 2. SEM photographs of (a) RIE etched facets on c-plane sapphire test structures and (b) cleaved facets on a-plane sapphire.

stripes were formed in the center of these large mesas with widths ranging from 3 to 20 μm . A 0.1- μm etch was performed around the p-contact. Pad metal was deposited to provide a larger p-contact for ease in testing. The n- and p-contacts were formed by electron beam evaporation of Ti-Al-Ni-Au and Ni-Au, respectively.

Electrical testing was done using pulses of 20–200 ns with a 10-kHz pulse repetition frequency (duty cycle of 0.02%–0.2%). Data was taken using 0.02% duty cycle unless otherwise indicated. Pulses were generated by an Avtech AVR-C pulse generator driven by an HP 8116A pulse/function generator. A silicon photodiode was used as the detector. Light output power, current, and voltage were sampled in time with a Tektronix 11402 sampling oscilloscope. Spectral data was time averaged using an ANDO AQ-6315E optical spectrum analyzer with a resolution of 0.05 nm. The testing stage was equipped with a thermoelectric cooler allowing for temperature dependent measurements from RT up to 100 $^{\circ}\text{C}$.

III. RESULTS AND DISCUSSION

X-ray $2\Theta/\omega$ (004) rocking curves show superlattice peaks associated with the InGaN-InGaN:Si MQW region indicating high structural quality. The X-ray data were used to calculate alloy compositions and the MQW period. Strained layers were assumed as X-ray mapping indicates that these films are pseudomorphically strained.

Fig. 2 shows scanning electron microscope images of the facets for: (a) c-plane and (b) a-plane laser diodes. The c-plane facet shows some roughness associated with the RIE

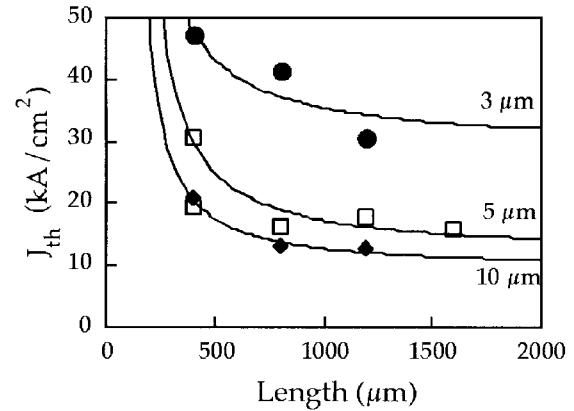


Fig. 3. Threshold current densities for pulsed operation (duty cycle = 0.02%) of RIE etched facet laser diodes with undoped wells of varying widths as a function of length.

etch as well as an angle approximately 6° off-vertical. These factors reduce the mirror reflectivity below the theoretical value (based on index refraction) of approximately 18%. The a-plane facet for the GaN epitaxial layers, shown in Fig. 3(b), appears fractured while the sapphire is smooth. The facet cleaved along the sapphire r-plane and fractures the GaN layers. This fracturing is caused by a 2.4° misorientation between the crystal planes. This mismatch occurs because the a-plane of the GaN orients along the c-plane of the sapphire during growth. The r-plane is 57.6° from the c-plane in a-plane sapphire, while the a-planes are distributed every 60° in the GaN. The use of c-plane sapphire will be investigated to improve the facet quality of cleaved lasers.

Laser diodes were tested under pulsed conditions of 20-ns pulses with 10-kHz repetition frequency (duty cycle = 0.02%). The threshold current densities of the different structures were compared. There were two samples grown with Al compositions of 0.06 and 0.10. These samples showed similar threshold current densities. The structures with silicon doped quantum wells (on c-plane sapphire) showed considerably higher threshold current densities than the undoped quantum wells. The lowest threshold current density achieved with silicon doped wells was 18 kA/cm^2 versus 12.6 kA/cm^2 without doping. The a-plane sapphire sample with doped wells showed slightly lower threshold current densities (15 kA/cm^2) than the c-plane sample. This suggests that the cleaved facet laser outperforms the etched facet laser however there is a large scatter in the threshold current density and a limited number of data points. The samples with undoped quantum wells and 0.10 mole fraction of aluminum on c-plane sapphire and the doped quantum wells on a-plane sapphire were further investigated. Further discussion is on the c-plane sapphire structure unless otherwise indicated.

Diodes of different lengths and widths gave a range of threshold current densities as shown in Fig. 3. This data is for uncoated RIE etched facets. There was a considerable spread of threshold current densities for the devices. This plot shows the best threshold current density for each size tested. A reduction in threshold current density is observed with increasing width and length. The decrease with width is attributed to a reduction in carrier diffusion losses and/or

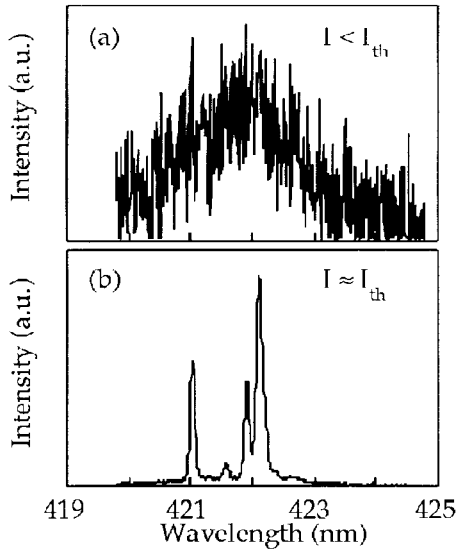


Fig. 4. Spectrum for $10 \times 800 \mu\text{m}$ RIE etched facet laser diode under pulsed operation (a) below threshold and (b) above threshold.

current spreading resulting in a pumped area larger than the contact size. The threshold current density levels off with increasing length due to the dominance of internal losses over mirror losses. This data was fit using (1). The prefactor in this fit is the threshold current density neglecting

$$J_{\text{th}} = J_{\text{th},\infty} \cdot \exp\left(\frac{L_0}{L}\right) \quad (1)$$

mirror losses ($L \rightarrow \infty$) which decreases from 28 to 9.2 kA/cm^2 for the 3 and $10\text{-}\mu\text{m}$ -wide stripes, respectively. The lowest threshold current density observed experimentally was 12.6 kA/cm^2 for a $10 \times 1200\text{-}\mu\text{m}$ laser bar with uncoated facets at room temperature (RT).

Spectra were collected above and below threshold. Below threshold a broad spontaneous emission spectrum with no resolved modes is evident, Fig. 4(a). Just above threshold, a strong mode spectrum appears, as shown in Fig. 4(b). The width of the observed peaks corresponds to the analyzer resolution (0.05 nm). The resolution is not sufficient to resolve the expected individual mode spacing for the cavity lengths tested. Spectra were taken for devices with different stripe-width laser diodes. We observed no correlation between the stripe width and the peak spacing as would be seen for lateral modes. These spectra showed a maximum occurrence of a 0.35-nm peak spacing which is similar to that observed by Nakamura [1]. The origin of this modulation has been reported to arise from a self-pulsation phenomenon [9].

A near-field image of a cleaved facet laser diode is shown in Fig. 5. Fig. 5(a) is for below threshold operation. One can see a broad emission region for the spontaneous emission. Above threshold, Fig. 5(b), a central spot is evident indicating a gain guided optical beam. In the direction perpendicular to the quantum-well plane, a double lobe structure is evident. We believe this is due to the two competing waveguides in the structure, the InGaN MQW active region clad by AlGaIn and the GaN:Si region clad by AlGaIn and sapphire. This indicates a leaky waveguide that increases intrinsic loss and limits

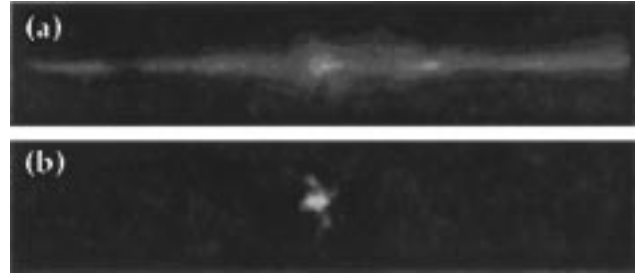


Fig. 5. Near-field of cleaved facet laser diode (a) below threshold and (b) above threshold under pulsed operation.

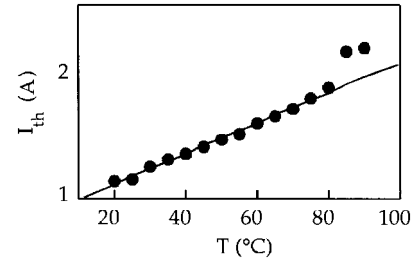


Fig. 6. Threshold current rise versus temperature for a $3 \times 1200 \mu\text{m}$ RIE etched facet laser under pulsed operation (duty cycle = 0.02%).

device performance. This effect will be more significant for the RIE etched facet lasers because the facet only extends through the AlGaIn cladding regions causing the light propagating in the GaN:Si to be lost.

Thermal characteristics were determined by heating the testing stage with a thermoelectric cooler for low duty cycle pulsed operation. This sample ($3 \times 1200 \mu\text{m}$) operated up to a maximum temperature of $95 \text{ }^\circ\text{C}$. Between $80 \text{ }^\circ\text{C}$ and $85 \text{ }^\circ\text{C}$, the sample experienced a partial short through the active region causing a large increase in threshold current. The threshold current plotted versus temperature was fit to the characteristic temperature formula (2) yielding a T_0 of 114 K , shown in Fig. 6.

$$I_{\text{th}} = I_{\text{th},0} \cdot \exp\left(\frac{T}{T_0}\right). \quad (2)$$

The light output versus current ($L-I$) dependence on pulse-length for a $5 \times 1200 \mu\text{m}$ device is shown in Fig. 7. The longer pulse-lengths cause an increase in heating which is evidenced through the increase in the threshold current. This sample operated for a pulse-length of up to 150 ns at 10 kHz . The $L-I$ curves were relatively insensitive to the operation frequency for these short pulse-lengths. The rise in current with pulse-length can be used to estimate the junction temperature using the characteristic temperature. A temperature rise of $90 \text{ }^\circ\text{C}$ is estimated for 114 K characteristic temperature.

As mentioned, the heating in these devices is considerable. The heating is determined by the current density and voltage. These devices showed relatively high voltage levels, between $19\text{--}30 \text{ V}$. The majority of this voltage is likely associated with the p-contact, p-bulk layers, and possibly n-contact spreading resistance. The device voltage is obtained by subtracting an inductive probe resistance.

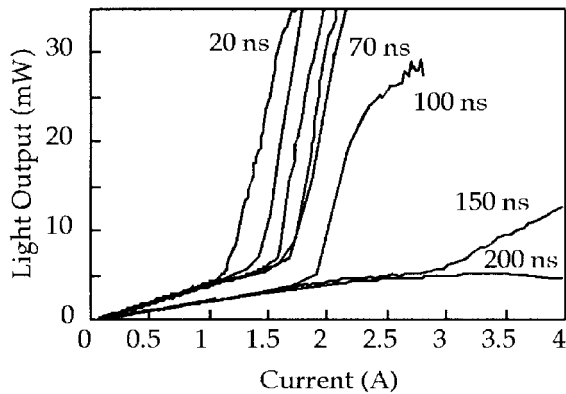


Fig. 7. Light output for pulsed operation at different pulselengths with a frequency of 10 kHz (duty cycle: 0.02%–0.2%) at RT for a $5 \times 1200 \mu\text{m}$ RIE etched facet laser diode.

A $10 \times 400 \mu\text{m}$ laser bar was operated above threshold ($P_0 = 10 \text{ mW}$ per facet) under pulsed conditions to estimate the lifetime. L – I measurements were performed at 1-h intervals to determine the degradation with time. After 1 h of operation, the threshold current improved. This could be due to further thermal activation of the acceptors or contact alloying. The threshold current steadily increased over the next 5 h. After 8.5 h of testing, the sample no longer lased. The current voltage characteristics indicated a short had formed which is the dominant failure mechanism observed.

IV. CONCLUSION

Pulsed operation of 420-nm blue laser diodes for RIE etched and cleaved facets with threshold current densities as low as 12.6 kA/cm^2 was achieved. Samples without doping in the quantum wells show higher performance than silicon-doped wells. Near-field of cleaved facet lasers show a double-lobed pattern indicated light propagating in the GaN:Si layer. The devices operated up to a maximum ambient temperature of $95 \text{ }^\circ\text{C}$ and pulselengths up to 150 ns. Lifetimes in excess of 6 h have been demonstrated. The performance of these devices is limited by resistive heating during the pulses and leaky waveguides.

REFERENCES

- [1] S. Nakamura and G. Fasol, *The Blue Laser Diode*. Berlin, Germany: Springer-Verlag, 1997.
- [2] K. Itaya, M. Onomura, J. Nishio, L. Sugiura, S. Saito, M. Suzuki, J. Rennie, S. Nuonee, M. Yamamoto, H. Fujimoto, Y. Kokubun, Y. Ohba, G. Hatakoshi, and M. Ishikawa, "Room temperature pulsed operation of nitride based multi-quantum-well laser diodes with cleaved facets on conventional C-face sapphire substrates." *Jpn. J. Appl. Phys.*, vol. 35, no. 10B, pp. L1315–L1317, 1996.
- [3] I. Akasaki, S. Sota, H. Sakai, T. Tanaka, M. Koike, and H. Amano, "Shortest wavelength semiconductor laser diode," *Electron. Lett.*, vol. 32, no. 12, pp. 1105–1106, 1996.
- [4] A. Kuramata, K. Domen, R. Soejima, K. Horino, S. Kubota, T. Tanashi, "InGaN laser diode grown on 6H-SiC substrate using low-pressure metal organic vapor phase epitaxy," *Jpn. J. Appl. Phys.*, pt. 2 (*Lett.*), vol. 36, no. 9A-B, pp. LL1130–LL1132, 1997.
- [5] G. E. Bulman, K. Doverspike, S. T. Sheppard, T. W. Weeks *et al.*, "Pulsed operation lasing in a cleaved-facet InGaN/GaN MQW SCH laser grown on 6H-SiC" *Electron. Lett.*, vol. 33, no. 18, pp. 1556–1557, 1997.
- [6] M. P. Mack, A. C. Abare, M. Hansen, P. Kozodoy, S. Keller, U. Mishra, L. A. Coldren, and S. P. DenBaars "Room temperature pulsed

operation of blue nitride based laser diodes," in *Proc. Int. Conf. Nitride Semiconductors*, 1997, p. 459, paper LN-7.

- [7] M. Kneissl, D. Hofstetter, D. P. Bour, R. Donaldson, J. Walker, and N. M. Johnson, "Dry-etching characterization of mirrors of III-nitride laser diodes from chemically assisted ion beam etching," in *Proc. Int. Conf. Nitride Semiconductors*, 1997, pp. 462–463, paper S-6.
- [8] F. Nakamura, T. Kobayashi, T. Asatsuma, K. Funato, K. Yanashima, S. Hashimoto, K. Naganuma, S. Tamioka, T. Miyajima, E. Morita, H. Kawai, and M. Ikeda, "Room temperature pulsed operation of a GaInN multiple-quantum-well laser diode with an optimized well number," in *Proc. Int. Conf. Nitride Semiconductors*, 1997, p. 460, paper LN-8.
- [9] PR Newswire, SDL Inc., Feb. 13 1998.
- [10] S. Nakamura, M. Senoh, S. Nagahama, N. Iwasa, T. Yamada, T. Matsushita, H. Kiyoku, Y. Sugimoto, T. Kozaki, H. Umemoto, M. Sano, and K. Chocho, "Present status of InGaN/GaN/AlGaIn-based laser diodes," in *Proc. Int. Conf. Nitride Semiconductors*, 1997, pp. 444–446, paper S-1.
- [11] R. K. Sink, A. C. Abare, P. Kozodoy, M. P. Mack, S. Keller, L. A. Coldren, S. P. DenBaars, and J. E. Bowers "Pulsed operation of cleaved-facet InGaN laser diodes," in *Proc. Mater. Res. Soc.*, Fall Meet., Boston, MA, 1997, paper D22.1.

A. C. Abare, photograph and biography not available at the time of publication.

M. P. Mack, photograph and biography not available at the time of publication.

M. Hansen, photograph and biography not available at the time of publication.

R. K. Sink, photograph and biography not available at the time of publication.

P. Kozodoy, photograph and biography not available at the time of publication.

S. Keller, photograph and biography not available at the time of publication.

J. S. Speck, photograph and biography not available at the time of publication.



J. E. Bowers (S'78–M'81–SM'85–F'93) received the M.S. and Ph.D. degrees in applied physics from Stanford University, Stanford, CA.

He is the Director of the Multidisciplinary Optical Switching Technology Center (MOST) and a Professor in the Department of Electrical Engineering, University of California, Santa Barbara. He is a member of the Optoelectronics Technology Center and the NSF Science and Technology Center on Quantized Electronic Structures. His research interests are primarily concerned with high-frequency optoelectronic devices and physics. He has worked for AT&T Bell Laboratories and Honeywell before joining UCSB. He has published five book chapters, over 200 journal papers, over 200 conference papers, and has received 12 patents.

Dr. Bowers is a Fellow of the American Physical Society, a recipient of the IEEE LEOS William Streifer Award, and is Vice President for Conferences of IEEE LEOS. He is a recipient of Sigma Xi's Thomas F. Andrew prize and the NSF Presidential Young Investigator Award and NSF Graduate Fellowship.

U. K. Mishra, photograph and biography not available at the time of publication.

S. P. DenBaars, photograph and biography not available at the time of publication.



L. A. Coldren (S'67–M'72–SM'77–F'82) received the Ph.D. degree in electrical engineering from Stanford University, Stanford, CA, in 1972.

After 13 years in the research area at Bell Laboratories, he was appointed Professor of Electrical and Computer Engineering (ECE) at the University of California, Santa Barbara (UCSB) in 1984. In 1986, he assumed a joint appointment with Materials and ECE. At UCSB, his efforts have included work on novel guided-wave and vertical-cavity modulators and lasers as well as the underlying materials growth and dry-etching technology. He is currently investigating the integration of various high-speed optoelectronic devices, including optical modulators, tunable lasers, and surface-emitting lasers. He is also heavily involved in new materials growth and fabrication technology essential to the fabrication of such integrated optoelectronic components. His group has made many seminal contributions in these areas, including recent contributions in ultrawide-tuning-range lasers with good spurious mode suppression, vertical-cavity lasers with high efficiency, high power, and temperature insensitivity, and UHV *in situ* etching and regrowth. He has authored or coauthored over 300 papers, three book chapters, and one textbook, and has been issued 26 patents. He is currently Director of the multicampus ARPA-supported Optoelectronics Technology Center.

Dr. Coldren is a Fellow of the Optical Society of America, a past Vice-President of IEEE Lasers and Electro-Optics Society, and has been active in technical meetings.